ACS Catalysis

RESEARCH ARTICLE

pubs.acs.org/acscatalysis

Low Temperature Water Gas Shift: Evaluation of Pt/HfO_2 and Correlation between Reaction Mechanism and Periodic Trends in Tetravalent (Ti, Zr, Hf, Ce, Th) Metal Oxides

Mauro C. Ribeiro, Gary Jacobs, Linda Linganiso, Khalid G. Azzam, Uschi M. Graham, and Burtron H. Davis*

Center for Applied Energy Research, University of Kentucky, 2540 Research Park Dr., Lexington, Kentucky 40511, United States

ABSTRACT: It is well-known that catalysts containing small quantities of noble metals (e.g., Pt, Au) that are highly dispersed on Group IV and related tetravalent metal oxides (e.g., TiO_2, ZrO_2, CeO_2, ThO_2) display, once activated, high conversion for water-gas shift (WGS). The mechanism suggested for this by many authors is bimolecular in nature. In one view, adsorption of CO on the partially reducible oxide produces formates by reaction with active bridging OH groups, followed by water-assisted formate decomposition by dehydrogenation, with this second step being facilitated by metal particles at the metal−support interface. Considering this group of oxides, HfO_2, as far as we are aware, had not yet been studied as a potential candidate for low temperature water-gas shift (LTWGS). Thus, in this contribution, catalysts composed of Pt supported on HfO_2 were prepared and tested. Catalyst testing results suggest that this system is, like Pt/ZrO_2 and Pt/CeO_2, active for the WGS reaction, although additional studies are required to obtain an ordering of reactivity. Insight into the possible mechanism was gained through the use of diffuse reflectance infrared Fourier transform spectroscopy (DRIFTS). Formate bands were observed to form when defect-associated bridging OH groups, present on hafnia after partial reduction, were reacted with CO. Pt facilitated partial reduction of hafnia and thus the formation of the bridging OH groups on its surface. The formate bands readily disappeared in the presence of steam at 130 °C, converting to the second intermediate, carbonate species, which liberated CO_2 and presumably H_2 products. Moreover, in switching from CO adsorption alone to steady state LTWGS, the formate bands became reaction rate limited—and more so at higher temperature. The implication is that formate is turning over more rapidly at the latter condition, with its decomposition (probably via C−H bond breaking) being the most likely rate limiting step. These experiments suggest that the reaction probably follows a bimolecular associative pathway, with adsorbed formate being an intermediate, in the same manner as observed with the other Group IV and related tetravalent oxide based LTWGS catalysts. Moreover, an interesting relationship may exist between the C−H bond strength of adsorbed formate (i.e., observed during CO adsorption) and the metal ion radius in the oxide.

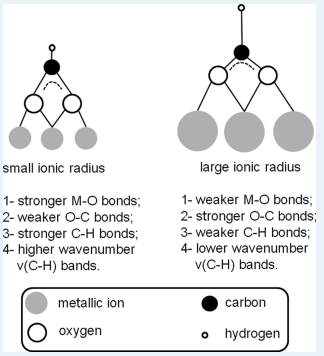

KEYWORDS: hafnia, Pt/HfO_2, WGS, LTS, Group IV, tetravalent oxides

1. INTRODUCTION

The water-gas shift (WGS) reaction, represented by the following equilibrium $CO+H_2O \leftrightarrow CO_2+H_2$ ($\Delta H^0 = -41.2$ kJ mol^{-1}), is important for generating and purifying H_2, a necessary feedstock for many important processes.[1] It is carried out in both high (350−450 °C) and low temperature (180−300 °C) ranges within a fuel processor for fuel cell applications. The high temperature water-gas shift (HTWGS) step is typically carried out over a magnetite/chromia based catalyst which is intended to remove CO at high rates. However, the exothermicity of the reaction limits the thermodynamic equilibrium conversion at high temperatures; thus, catalysts that are active in the low temperature range are used in the final stage. The typical $Cu/ZnO/Al_2O_3$ catalyst used commercially is pyrophoric and thus not amenable to the rapid startup/shutdown steps occurring in a fuel processor used for fuel cell applications. Thus, a nonpyrophoric catalyst with high activity at low temperatures is needed to decrease the CO content to below 0.3% wt.,[1] where the trace levels may be handled by selective oxidation. One family of catalysts that is being actively investigated is that consisting of a partially reducible oxide (PRO) (e.g., ceria or zirconia) with supported noble metal particles (e.g., Pt, Pd, Au). The metallic centers are suggested to play the dual role of facilitating the partial reduction of the PRO as well as participating in the mechanism.[2,3] Basically there are two popular viewpoints regarding the WGS mechanism. The first class of mechanism is known as the *redox* mechanism, where CO adsorbed on Pt associates with oxygen adsorbed on the PRO at the interface between the metallic particle and the PRO and is released as CO_2, leaving an oxygen vacancy in the surface of the PRO. The oxygen vacancy is then replenished by reduction of water, yielding H_2. There is convincing evidence that this mechanism may take place in HTWGS catalysts like magnetite/chromia, and some have suggested, based on kinetic data, that it may occur with LTWGS catalysts like Pt/ceria.[4,5]

Received: May 6, 2011
Revised: July 13, 2011
Published: August 29, 2011

However, it has been questioned whether H_2O can decompose at oxygen vacancies at the PRO to deposit an O adatom and generate H_2 at such low temperatures. Many have argued in favor of a different bimolecular mechanism. That is, instead of H_2O activation involving reoxidation of the support with liberation of H_2, others have proposed that H_2O dissociates at the vacancies to generate active Type II bridging OH groups. These, in turn, are proposed to form associated intermediates (e.g., formates) by reaction of the bridging OH group with CO. Shido and Iwasawa provided detailed infrared spectroscopic investigations of ceria and Rh/ceria that revealed that bidentate formates were formed on partially reduced ceria by the association of active OH groups, and that their decomposition in the forward direction (i.e., to H_2 and CO_2, the latter by way of unidentate carbonate) was facilitated by coadsorbed H_2O.[6] These authors also identified a kinetic isotope effect (KIE) during WGS by H-D switching and correlated this KIE to that observed in C−H bond breaking of formate when formate was exposed to steam. Thus, they could infer that C−H breaking was likely the rate determining step of the catalytic cycle. Virtually the same KIE was observed by Jacobs et al.[7,8] for Pt/ceria catalysts (i) during WGS, (ii) during steam-assisted formic acid decomposition,[9] (iii) during transient decomposition of formate[7] when exposed to steam at low temperature (i.e., where both steam and formate were labeled by H and D), and (iv) during monitoring of the coverage response of formate[8] when switching from CO adsorption to steady state shift. In the latter case, the coverage of H-labeled formate was examined when exposed to H_2O and compared to that of the D-labeled formate when it was exposed to D_2O. Following the proposal of this view, Pigos et al. presented infrared spectroscopy evidence that formate C−H bond weakening was attained by alkali doping,[10] which could explain the acceleration of the WGS rate over Na-doped Pt-ZrO_2 catalysts.[7]

Active catalysts for LTWGS are often composed of a noble metal dispersed on a PRO like TiO_2,[11−13] ZrO_2,[14−16] CeO_2,[2−9] or ThO_2.[17−19] Interestingly, the metal centers in all these oxides, prior to activation by surface shell reduction, are tetravalent ions; furthermore, tetravalent ions remain in the core of the oxide even after activation. Another interesting similarity is that there is mounting evidence that LTWGS takes place in catalysts based on these oxides according to the associative pathway, with formate as an intermediary and with the C−H bond breaking as the rate determining step,[3] rather than following the redox pathway. Besides Ti, Zr, and Hf, Ce and Th display resemblances to the Group IV oxides, as they can present a stable 4+ valence[20] and a similar chemistry (e.g., "masquerading" as a Group IV oxide[21]), in spite of certain differences in valence level electronic structure. Laing[22] has even gone so far as to propose an extended Group IV column containing, among others, ceria and thoria, the latter of which was placed in Group IV as late as the 1920s, because of its similar chemistry to hafnia.[23] It should be emphasized, however, that the proposed surface involved in the catalysis of LTWGS does not involve the fully oxidized tetravalent metal oxide, but a defect-laden surface consisting of reduced centers (i.e., bridging OH groups associated with oxygen vacancies); the internal structure (i.e., the core of the oxide) containing the M^{4+} electronic structure is necessary, however, for sustaining the defects in the outer shell. Evidence from X-ray absorption near edge structure (XANES) spectroscopy reveals that activated ceria possesses both Ce^{4+}, presumably in the core, and Ce^{3+}, in the surface shell.[24−26] Note that diffuse reflectance infrared Fourier transform spectroscopy (DRIFTS) confirms that bridging OH groups, associated with Ce^{3+} defects, are formed; thus, Ce^{3+} can be assigned to the surface shell of the oxide.

Table 1. BET Surface Area and Porosity Measurements from Physisorption of Nitrogen at 77 K

catalyst description	BET SA (m^2/g)	average pore volume (cm^3/g)	average pore radius (nm)
HfO_2	140	0.075	1.3
0.5% Pt/HfO_2	127	0.077	1.3
1% Pt/HfO_2	126	0.075	1.3
2% Pt/HfO_2	127	0.069	1.4
ZrO_2	142	0.23	2.3
2% Pt/ZrO_2	137	0.22	2.6
CeO_2	122	0.102	1.70
0.5% Pt/CeO_2	117	0.103	1.72
1% Pt/CeO_2	114	0.101	1.74

Elements from the same group have an increase in their atomic/ionic radius as new quantum levels are being occupied. As a consequence, the density of charge (Coulombic charge to mass ratios) decreases for the larger metallic ions. The basicity of metal hydroxides, which is inversely proportional to the metal−oxygen bond strength, tends to increase with the radius of the metallic ion;[28] this means that weaker metal−oxygen bonds could be expected in moving from the oxides/hydroxides of Ti^{4+} to Th^{4+}. Although this family of metal oxides has similarities in structure and stoichiometry (arising from the assumption that one may choose to classify these metallic ions in the same periodic group), they possess differences in metal−oxygen bond strengths, which depend on their crystalline ionic radii. Furthermore, these differences can affect the manner in which molecules adsorb on their surfaces, once activated. To probe this influence on metal/PRO catalysts for LTWGS, DRIFTS may be a useful tool to correlate catalyst activity to the possible mechanism and specifically, the influence of the catalyst surface structure on the adsorption and reaction of intermediates.[3] As far as we are aware, hafnia has not yet been studied as a PRO support for WGS. Therefore, the aim of the present work is to complete the Group IV metal oxides by investigating whether Pt/HfO_2 is active for WGS and, if so, the likelihood that an associative formate mechanism may apply, as has been suggested in the case of the other Pt-containing Group IV and related tetravalent metal oxides. Another aim of this work is to examine the possibility of a periodic relationship between the formate C−H bond frequency and ionic radius of the metal among the Group IV and related tetravalent metal oxides.

In this contribution, Pt/HfO_2 catalysts were prepared and characterized by temperature programmed reduction (TPR), X-ray diffraction (XRD), transmission electron microscopy (TEM), and N_2 physisorption. Catalytic tests were undertaken to evaluate the catalytic activity under relevant LTWGS conditions. To characterize the surface chemistry of the catalysts, DRIFTS experiments were also conducted. Results were correlated with those obtained previously from the Pt/TiO_2,[3] Pt/ZrO_2,[10] Pt/CeO_2,[26] and Pt/ThO_2[17] systems. An interesting relationship appears to exist between the strength of the C−H bond of formate and the ionic radius for the solid.

2. EXPERIMENTAL SECTION

2.1. Catalyst Preparation. For the preparation of the HfO_2 support, $HfCl_4$ (Aldrich) was slowly dissolved in deionized (D.I.)

dx.doi.org/10.1021/cs200231h |ACS Catal. 2011, 1, 1375–1383

water, so that a final concentration of 0.1 mol L^{-1} of Hf (IV) was reached. Afterward, urea was added in a Hf/urea molar ratio of 1:40, to ensure quantitative precipitation of Hf (IV). After 90 h of reflux at 95 °C under magnetic stirring, the precipitate was collected by filtration and the solid white gel was resuspended in 800 mL of boiling water, left for 30 min of refluxing, and then refiltered again. This operation was repeated until achieving a negative response with a 2 mol L^{-1} $AgNO_3$ solution, which was accomplished after washing 12 times. After a negative test for Cl^-, suspension, reflux, and filtration were repeated a further two times. The washed gel was then dried for 12 h at 120 °C, crushed, sieved in the 80 < Φ < 230 μm particle size range, and then calcined at 400 °C for 5 h. The high surface area powder obtained (130 m^2 g^{-1}) was doped with Pt by incipient wetness impregnation (IWI) using a solution containing the proper quantity of $Pt(NH_3)_4(NO_3)_2$ (Aldrich 99%). After impregnation, the mixture was dried at room temperature overnight and then calcined at 350 °C for 4 h. The ceria and thoria oxides were prepared by precipitation of the nitrates using urea[5] to slowly release the hydroxide anion, as described elsewhere;[26,27] calcination of the resulting hydroxides led to oxide surface areas of 125 and 165 m^2/g for ceria and thoria, respectively. A commercial high surface-area zirconia support from Gobain NorPro (Brunauer–Emmett–Teller (BET) surface area of 142 m^2/g) was used. The titania was also a commercial support, with a surface area of 41 m^2/g. Elemental analysis of catalysts verified that Pt loadings prepared using the IWI technique were within 2% of nominal loadings.

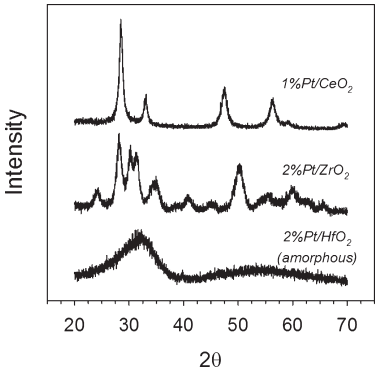

Figure 1. XRD profiles of Pt loaded ceria, zirconia, and hafnia samples used in this study.

2.2. Catalyst Characterization

2.2.1. BET Surface Area and Porosity. BET measurements were carried out on both calcined HfO_2 and Pt/HfO_2 catalyst precursors using a Micromeritics Tri-Star system. Prior to measurement, the sample was heated to 160 °C, evacuated to approximately 50 mTorr, and held at this condition overnight. The BET surface area, pore volume (single point and BJH adsorption), and average pore radius (single point) were obtained.

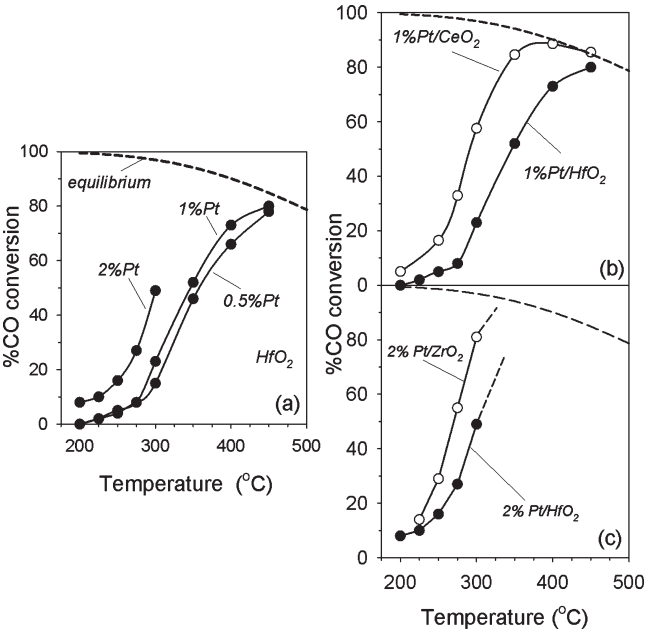

Figure 3. CO conversion as a function of reaction temperature (a) over HfO_2 with 0.5, 1.0, and 2.0% Pt loadings; (b) between 1%Ptceria and 1% Pt/hafnia; and (c) between 2%Pt/HfO_2 and 2%Pt/ZrO_2 catalysts. Gas composition (mol %): $CO/H_2O/N_2/H_2/He$ = 2.99/26.12/3.73/29.85/37.31. WHSV 84.75 SL h^{-1} g_{cat}^{-1}; pressure: 1 atm.

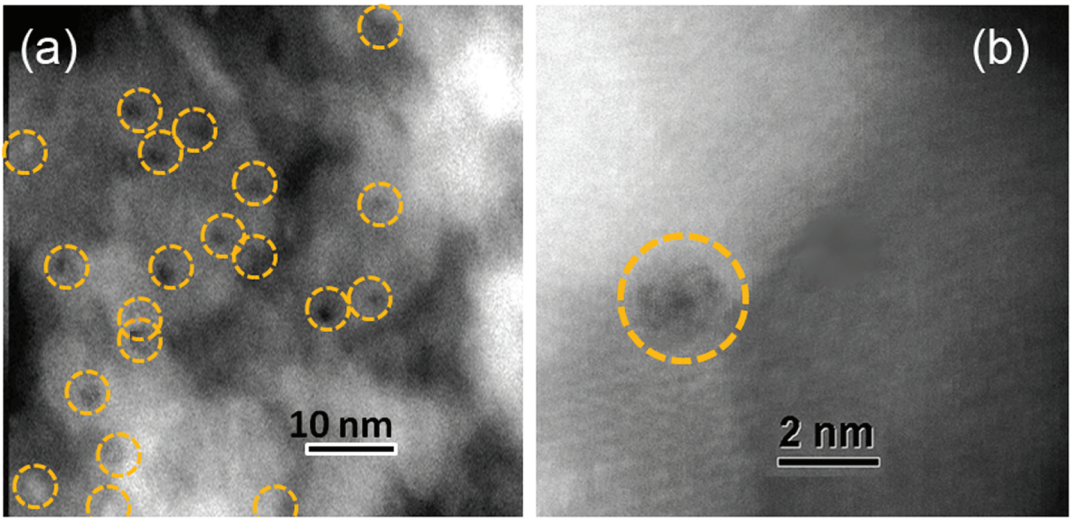

Figure 2. STEM images of reduced/passivated 2%Pt/ZrO_2. (a) Circles denote well-dispersed Pt nanoparticles ~2 nm, while panel (b) shows a zoom in on a typical Pt particle.

dx.doi.org/10.1021/cs200231h |ACS Catal. 2011, 1, 1375–1383

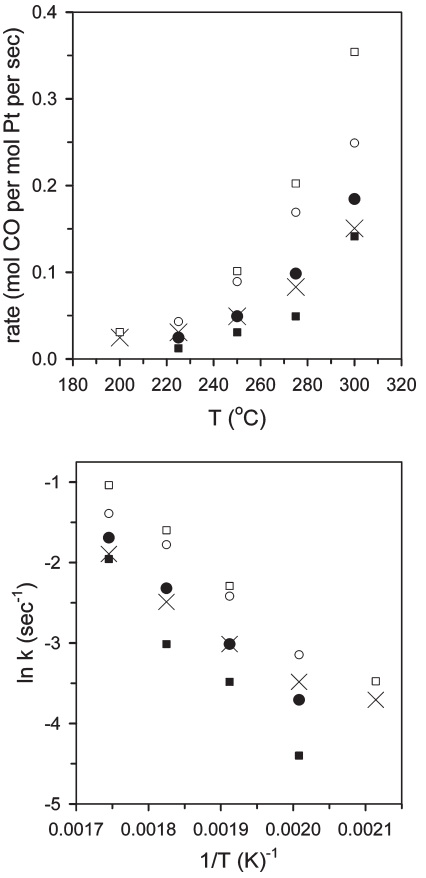

Figure 4. (top) Rate as a function of Pt content and (bottom) Arrhenius plots for (filled circles) 0.5%Pt/HfO_2; (filled squares) 1%Pt/HfO_2; (X's) 2%Pt/HfO_2; (open circles) 2%Pt/ZrO_2; and (open squares) 1% Pt/CeO_2.

2.2.2. XRD. X-ray diffraction (XRD) patterns were recorded using a Philips X'Pert diffractometer. The conditions were: scan rate of 0.025° per step, scan time of 5 s per step, and a 2θ range of 20−70°.

2.2.3. HRTEM. High resolution transmission electron microscopy (HRTEM) measurements were carried out using a JEOL 2010 TEM field emission electron microscope, equipped with an energy dispersive X-ray (EDX) detector, and operated at an accelerating voltage of 200 kV. Furthermore, Emisec Control is used for digital beam control and the integration of STEM (scanning transmission) images. The electron beam has a point-to-point resolution of 0.5 nm. Prior to HRTEM analysis the samples were reduced ex situ in flowing hydrogen at 350 °C and subsequently passivated at room temperature using 1% O_2 in helium. Catalyst powder was lightly dusted onto 200 mesh Cu grids coated with lacy carbon.

2.2.4. TPR. Temperature programmed reduction (TPR) was conducted on HfO_2 and 1%Pt/HfO_2 catalysts using a Zeton-Altamira AMI-200 unit equipped with a thermal conductivity detector (TCD). The temperature range was 50 to 1100 °C, and the ramp rate was 10 °C/min. Argon served as the reference gas, and 10%H_2 in Ar was used as the treatment gas. The flow rate of the H_2 treatment gas was 30 cm^3/min. The temperature of the catalyst was recorded from a thermocouple positioned inside the catalyst bed. Approximately 0.30 g of catalyst was utilized in each test.

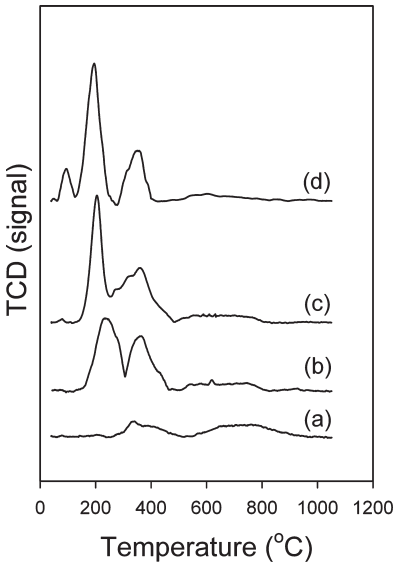

Figure 5. H_2-TPR of, moving upward, (a) HfO_2; (b) 0.5%Pt/HfO_2; (c) 1%Pt/HfO_2; and (d) 2%Pt/HfO_2 catalysts.

2.2.5. DRIFTS. The infrared spectrometer was a Nicolet Nexus 870, equipped with a DTGS-TEC detector. A chamber fitted with ZnSe windows capable of high temperature and high pressure served as the reactor for CO adsorption and WGS experiments. The gas lines leading to and from the reactor were heat traced and insulated with ceramic fiber wrap. Scans were taken at a resolution of 4 to give a data spacing of 1.928 cm^{-1}. For steady state measurements, 512 scans were taken to improve the signal-to-noise ratio and multiple scans were made to ensure reproducibility of the steady state condition. For transient measurements, however, 32 scans were required. The amount of catalyst was ∼40 mg.

Feed gases were controlled by Brooks 5850 series E mass flow controllers. Iron carbonyl traps consisting of lead oxide on alumina (Calsicat) were placed in the CO gas line. All gas lines were filtered with Supelco O_2/moisture traps. Catalysts were activated with 50 ccm of 33%H_2:He at 300 °C, purged in He, and cooled in He to a temperature of interest to obtain background scans. For CO adsorption measurements, CO:He (3.75 cm^3/min: 130 cm^3/min) was flowed at the temperature of interest. Following CO adsorption experiments, steady state water gas shift measurements were carried out (225 or 250 °C) using CO:H_2O:He 3.75 cm^3/min:62.5 cm^3/min:67.5 cm^3/min.

For transient formate decomposition experiments, following catalyst activation, background collection, and CO adsorption (225 °C), the catalyst was cooled to 130 °C in CO:He (3.75 cm^3/min: 130 cm^3/min). This was followed by a He purge (130 cm^3/min). Formate decomposition was followed (32 scans each spectrum) in H_2O:He (62.5 cm^3/min: 67.5 cm^3/min) until virtually complete decomposition of the formate was observed. The catalyst was then purged in He (130 cm^3/min).

2.3. Catalytic Tests. Catalytic tests for the WGS reaction were carried out using a stainless steel fixed-bed tubular reactor (0.5 in o.d.) under steady state conditions. Typically, the catalysts were pressed into pellets, crushed, and sieved to yield grains of 355−600 μm in diameter. A 200 mg catalyst sample was diluted with 1800 mg of glass beads (60−80 μm in size) and then packed over a layer of quartz wool. Using the glass beads ensured plug

dx.doi.org/10.1021/cs200231h |*ACS Catal.* 2011, 1, 1375–1383

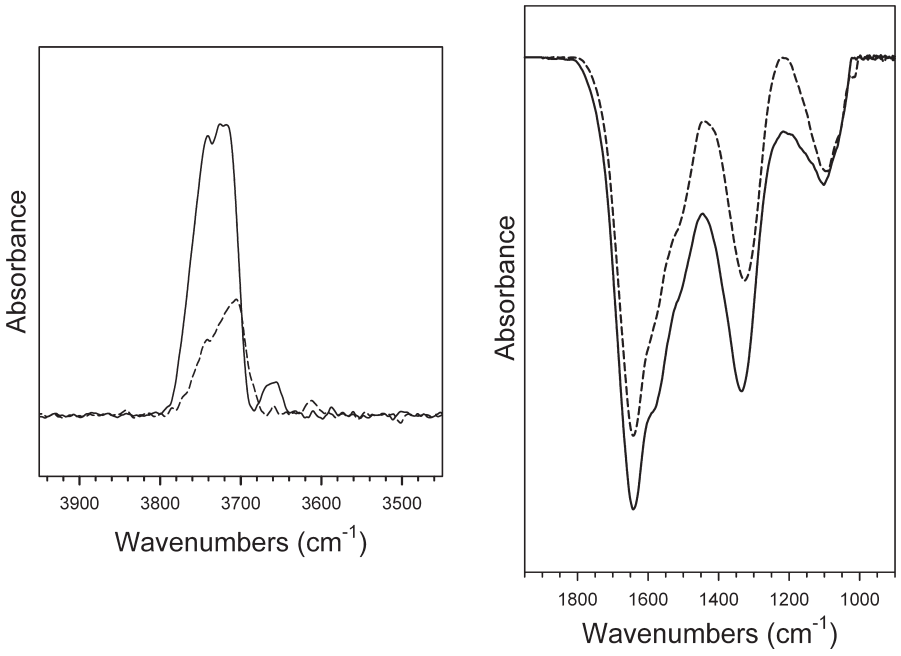

Figure 6. (left) Bridging OH groups formed and (right) decomposition of carbonate species over (dashed line) HfO_2 and (solid line) 1%Pt/HfO_2, after reduction in 50 ccm of 33%H_2/He at 300 °C.

Table 2. Proposed Band Assignments for Major Surface Species Observed by DRIFTS Spectroscopy after CO Adsorption, And during WGS Experiments

catalyst	activation	species	vibrational mode	band position
HfO_2, Pt/HfO_2	H_2 treated, CO + −OH	formation of formates	ν(C−H)	**2891**
			ν_{as}(OCO)	**1581**
			ν_s(OCO)	**1385**, 1373
			ν(C−H) +ν_s(OCO)	2978, 2966
			ν(C−H)	2750
	CO + H_2O H_2	formates	ν(C−H)	**2877** and **2846**
			ν(C−H) +ν_s(OCO)	2972
			ν(C−H)	2735
	H_2 treatment	decomposition of carbonates, carboxylates, or water	$\nu(CO_3)$ or ν(OCO) or ν(HOH)	**1637**, 1570, 1502, **1319**
	H_2 treated, (residual)	carbonates or carboxylates	$\nu(CO_3)$ or ν(OCO)	**1543**, **1390**; band range: 1700−1300
	H_2 treated, CO + Pt^0	Pt-CO	ν(CO)	linear **2042** (**max**), 2065 (shoulder) asymmetric bands 2085−1900
	H_2 treated, CO + −OH	OH (loss)	ν (O−H)	3728−3733, **3714**, 3670−3680
	formate decomp. in H_2O	carbonates or carboxylates formation, or water	ν (CO_3) or ν(OCO) or ν(HOH)	**1633**, **1590**, 1485, 1415, **1383**,

flow conditions and minimized the effect of heat generated by the mildly exothermic reaction. The temperature of the catalyst bed was monitored by a K-type thermocouple and was maintained by a temperature controller (Ω Omega CN 3251-R). All gases used (He, H_2, N_2, and CO_2) were of > 99.9% purity and of 99.5% purity for CO. Prior to testing, the catalysts were first reduced in H_2 (110 mL /min) at 350 °C for 1 h (ramp of 4 °C min^{-1}). A gas mixture containing 2.99 vol% CO, 26.12% H_2O, 29.85 vol % H_2,

dx.doi.org/10.1021/cs200231h |*ACS Catal.* 2011, 1, 1375–1383

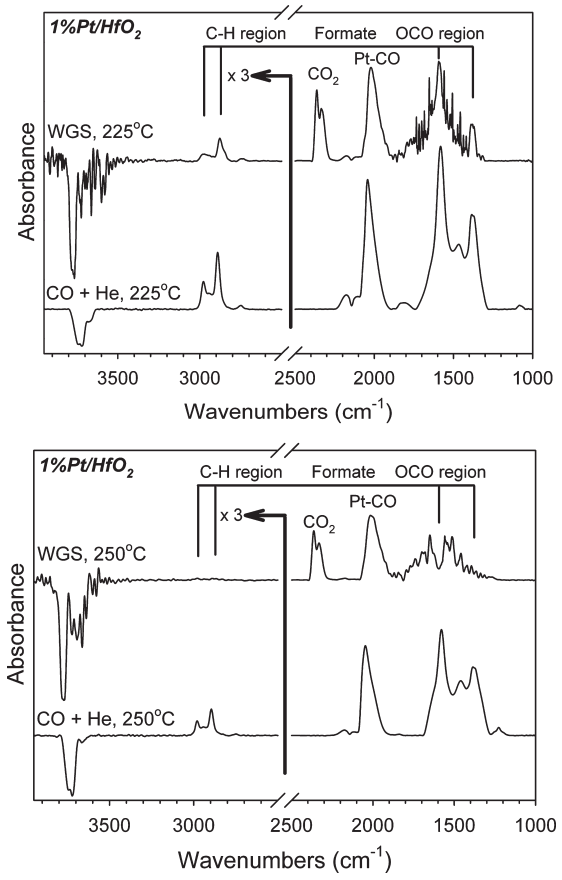

Figure 7. Steady state DRIFTS spectra of 1%Pt/HfO_2 at (top) 225 °C and (bottom) 250 °C, during (lower spectrum) CO adsorption using 3.75 ccm CO: 130 ccm He, and (upper spectrum) WGS using 3.75 ccm CO: 62.5 ccm H_2O: 67.5 ccm He.

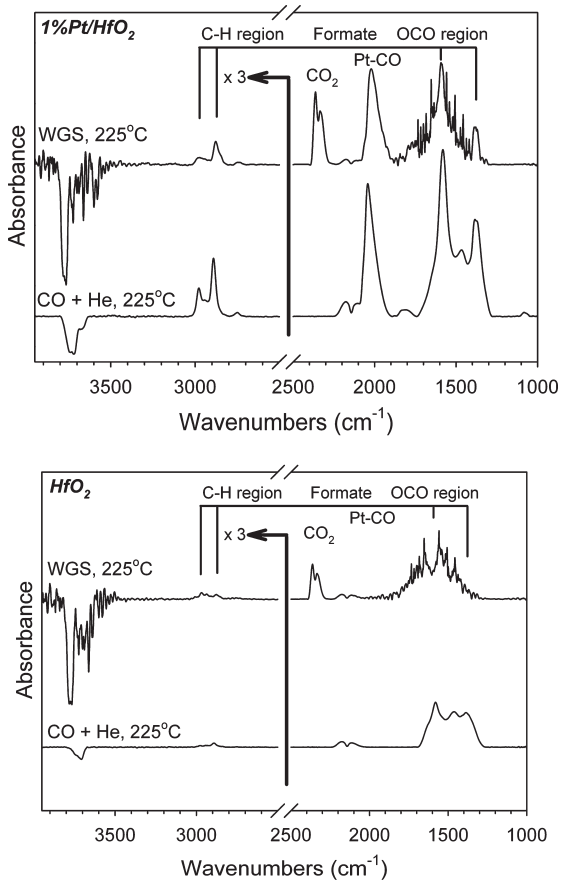

Figure 8. Steady state DRIFTS spectra at 225 °C of (top) 1%Pt/HfO_2 and (bottom) HfO_2, during (lower spectrum) CO adsorption using 3.75 ccm CO: 130 ccm He, and (upper spectrum) WGS using 3.75 ccm CO: 62.5 ccm H_2O: 67.5 ccm He.

3.73 vol %N_2 and He balance was used for catalytic tests. The dry gases were controlled using Brooks mass flow controllers. Steam was provided to the system via a steam generator consisting of a hollow cylinder (50 mm i.d., 150 mm long) packed with quartz wool. Water was fed by infusion with a syringe pump (Thermo scientific, model Orion M361) into the steam generator via a 1/16 in. needle having a side port hole. The whole system was heated to 180 °C to avoid condensation of H_2O. The feed was adjusted in bypass mode to obtain a constant $CO/H_2O/N_2/H_2$/He concentration prior to conducting the experiment (mol % = 2.99/26.12/3.73/29.85/37.31). Nitrogen was used as an internal standard. The products were passed though a cold trap, cooled to 0 °C, to condense water from the gas prior to analysis. The product gases were analyzed using a SRI 8610C Gas Chromatograph (SRI 8610C), which includes two columns (6′ silica gel packed and 3′ molecular sieve packed) and two detectors (FID and TCD). To boost the sensitivity of the CO and CO_2 signals, the GC incorporates a methanizer, such that these products can be analyzed by FID.

3. RESULTS AND DISCUSSION

Surface areas among the three supports tested were comparable, although HfO_2 presented a rather low pore volume (Table 1). According to Figure 1, unlike Pt/CeO_2 and Pt/ZrO_2, the hafnia sample is an amorphous powder even after two successive calcinations (i.e., first at 400 °C to form the oxide and second at 350 °C to decompose the Pt precursor). On the other hand, the presence of diffraction peaks due to reflection by (111) planes of both monoclinic and tetragonal phases, suggests that the sample may be a mixture of both phases. HR-TEM imaging indicated that, like the related oxides,[18,26,27] metal particles were below 10 nm (Figure 2). STEM images of the reduced/passivated 2%Pt/HfO_2 catalyst revealed (Figure 2a) well-dispersed Pt nanoparticles (Figure 2b) ∼2 nm in diameter.

Figure 3a displays the results of the catalytic testing of HfO_2 with different Pt loadings. The catalytic activity increases as the Pt loading increases. Jacobs et al.[26] reported higher CO conversion rates on a per gram catalyst basis with Pt/ceria catalysts and observed that, at the same temperature, the steady state formate coverage during LTWGS became more reaction rate limited (i.e., implying formate was turning over faster by forward decomposition) as a function of Pt loading. From these findings, the conclusion was drawn that Pt facilitates the dehydrogenation of formate (itself bound to the oxide by its O-atoms) at the metal-oxide interface. Transient formate decomposition experiments later revealed that not only the loading, but also the metal type impact the formate forward decomposition[29] and formate H-D exchange rates at the C−H bond.[30] The result suggests that, as in the case of Pt/ceria, the interaction between HfO_2 and Pt is important for WGS activity. Figures 2b and 2c show comparisons between catalytic activities of Pt/ceria and Pt/hafnia, and

dx.doi.org/10.1021/cs200231h |ACS Catal. 2011, 1, 1375–1383

Pt/zirconia and Pt/hafnia, respectively (note differences in Pt loadings). On a per gram catalyst basis (Figure 3) or per mole of Pt basis (Figure 4), the rates of the Pt/HfO_2 catalysts were within an order of magnitude of related materials. Again, although the surface areas among the three materials tested are comparable, HfO_2 presented a rather low pore volume. In the future, the material may be optimized to achieve a better performance. Apparent activation energies were assessed for data (Figure 4) between 225 and 275 °C. 0.5% and 1%Pt/hafnia, exhibited activation energies of ~63 kJ/mol, while that of 2%Pt/hafnia was somewhat lower, at 45 kJ/mol, while the reference 1% Pt/ceria and 2%Pt/zirconia catalysts had activation energies of ~62 kJ/mol (similar to activation energies reported by others[31]).

TPR profiles are reported in Figure 5. On the basis of infrared spectroscopy data for the reduction of the catalysts in H_2 (Figure 6), bridging OH group formation (Figure 6 left) and surface carbonate decomposition (Figure 6 right) are important steps during catalyst activation. Reduction of HfO_2 exhibited two distinct TPR peaks in the ranges of 300−500 °C and 570−900 °C, respectively. The peaks likely correspond to a surface reduction process involving both surface carbonate decomposition and uptake of hydrogen during formation of Type II bridging OH groups, as observed in the case of ceria.[32] The second peak may include loss of oxygen from the bulk lattice. The addition of Pt likely involves reduction of Pt oxide particles to Pt^0, but also causes a shift in the hafnia surface reduction process to a lower temperature; moreover, the second peak for bulk reduction appears to be lower in intensity. A major asymmetric peak is observed with maxima between 190 and at 235 °C, with pronounced shoulders in the range of 330−385 °C. With metal/CeO_2 catalysts, Jacobs et al.[26,27] observed that reduction of Pt oxide[26] or Au oxide[27] occurs first, at a temperature slightly lower than that of reduction of the surface layer of CeO_2. Pt therefore facilitates reduction of the hafnia surface shell, probably either via oxygen-vacancy formation and subsequent dissociation of H_2O to form the bridging OH groups, or directly by H_2 dissociation

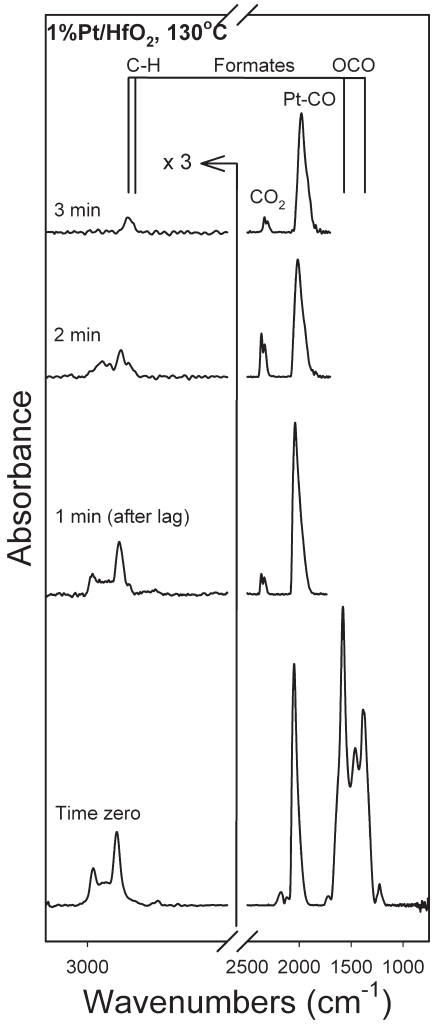

Figure 9. Transient DRIFTS spectra at 130 °C of 1%Pt/HfO_2 during following CO adsorption (3.75 ccm CO: 130 ccm He) and under formate decomposition with steam using 62.5 ccm H_2O: 67.5 ccm He.

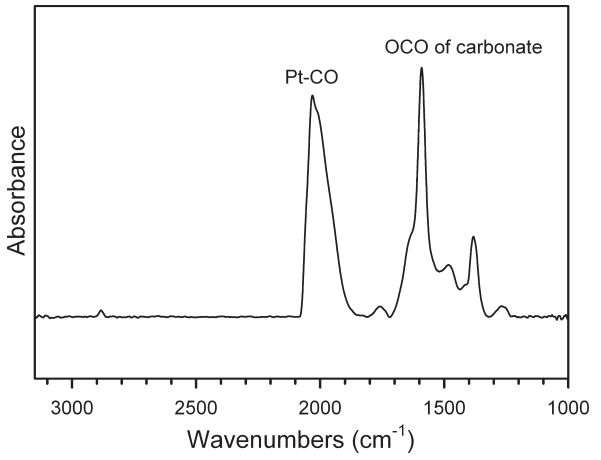

Figure 10. DRIFTS spectrum following formate decomposition (130 °C) and He purge (130 cm^3/min). Bands attributed to residual carbonates are observed.

Table 3. Comparison of the Main ν(C−H) among Activated Catalysts Containing Pt and an Activated Group IV Oxide

			ionic radius[a] (Å) [handbook]				
oxide	crystalline arrangement	CN	M^{3+}	M^{4+}	valence configuration[b]	ν(C−H) (cm^{-1})[c]	ref
TiO_2	tetragonal	6	0.67	0.61	$3s^23p^63d^24s^2$	2887	21
ZrO_2	monoclinic/tetragonal	8		0.84	$4s^24p^64d^25s^2$	2875	10
HfO_2	monoclinic/tetragonal	8		0.83	$5s^25p^65d^26s^2$	2890	
CeO_2	cubic (fluorite)	8	1.14	0.97	$4f^25s^25p^66s^2$	2845	14
ThO_2	cubic (fluorite)	8		1.05	$5f^26s^26p^67s^2$	2850	20

[a] Crystallographic ionic radii. [b] Valence configuration of the neutral elements. [c] Main C−H stretching wavenumber taken from previous work, cited in the references column.

dx.doi.org/10.1021/cs200231h |ACS Catal. 2011, 1, 1375–1383

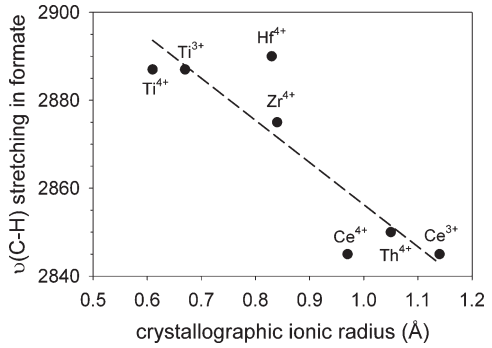

Figure 11. Relationship between adsorbed formate C−H band stretching energies and the crystallographic ionic radii of the different Group IV ion metals. Adsorbed formates were generated by CO adsorption on catalysts containing Pt and an activated Group IV metal oxide (see Table 3). The reference for ionic radii used is the *Handbook of Chemistry and Physics*, 90th ed.; D. L. Lide, Ed.; **2009**−**2010**, 12−11.

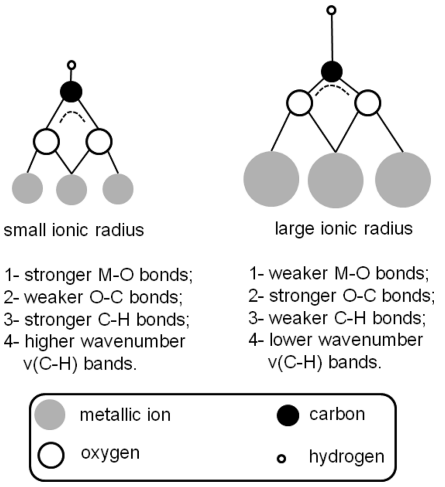

Figure 12. Sketch of the proposed model to explain the relationship between ν(C−H) stretching of adsorbed formate and the ionic radius of the Group IV metal oxide.

and spillover to the hafnia surface, as observed in the case of ceria activation. As with Pt/ceria catalysts observed previously,[26] increasing Pt loading causes a shift in peak maxima to lower temperatures (0.5%Pt, 235 °C; 1.0%Pt, 205 °C; 2.0%Pt, 192 °C); this has been explained in terms of the metal−support interaction. Higher loadings tend to generate larger metal crystallites that are easier to reduce because of a decrease in the surface interaction with the support.[26]

For ease of interpretation of infrared spectra, a summary of major band assignments is provided in Table 2. Upon reduction in H_2 of a 1%Pt/HfO_2 catalyst, CO_2 is generated and Pt-CO bands are formed during carbonate decomposition (Figure 6); residual carbonate bands change position. The main bands remaining on 1%Pt/HfO_2 are located at 1543 and 1390 cm^{-1}.

Results of CO adsorption at 225 and 250 °C after catalyst activation for HfO_2 and 1%Pt/HfO_2 catalysts are displayed in Figure 7. CO was observed to react with bridging OH groups (3733− 3680 cm^{-1} range) to generate bands attributed to surface formates. These bands included C−H stretching (ν(C−H) 2891, with minor bands of different modes at 2978, 2966, and 2750 cm^{-1}) and ν_{as}(OCO) asymmetric (1581 cm^{-1}) and ν_s(OCO) symmetric (1385, 1373 cm^{-1}) modes. 1%Pt/HfO_2 was observed to exhibit higher intensity formate bands versus unpromoted HfO_2. This is likely attributed to the role that Pt plays in facilitating the formation of reduced defect sites (e.g., Type II bridging OH groups[26] associated with vacancies[26] at low temperature. CO adsorption also resulted in the formation of Pt-CO bands assigned to linear ν(CO) (2065, 2042 cm^{-1}).

The formate species were found to be remarkably stable in the absence of steam at the temperatures typical of low temperature shift (i.e., 225− 250 °C) utilized in this work.

A comparison of numerous kinetic studies was made by Li et al.[5] At high H_2O/CO ratios, the rate of metal promoted, PROs (e.g., metal/ceria) has been suggested to be zero order in H_2O (i.e., whereby an adsorbed H_2O species is close to saturation), while that of CO is suggested to be first order, where the reaction rate essentially controls the coverage of the adsorbed CO intermediate.[5] It is not clear precisely where the switchover in order occurs, and additional kinetic investigations are needed. For example, Phatak et al.[31] reported zero order in P_{CO} even at 3:1 H_2O/CO, but the temperature used was considerably lower (∼200 °C), where the adsorbed CO intermediate species may still have been close to surface saturation. Here, we are carrying out experiments at higher temperatures, and much higher H_2O/CO ratios (∼17:1) in the presence of added H_2, which further promotes bridging OH group formation.[26] Thus, we cast our findings in terms of the switchover mechanism. In Figure 7, in switching from CO adsorption to WGS conditions (note partial pressure of CO remains unchanged), the formate coverage becomes reaction rate limited (i.e., suggesting formate is turning over rapidly), while the Pt-CO coverage remains relatively unchanged. This suggests that the adsorbed CO intermediate is likely the formate species. Moving from 225 to 250 °C, the formate band, which indicates significant coverage on the surface at 225 °C, becomes much more rate-limited at 250 °C, suggesting that the formate species is turning over more rapidly. Note that at 225 °C, there is a lower wavenumber (i.e., 2846 cm^{-1}) formate band that develops only during WGS (i.e., as opposed to CO adsorption). Shido and Iwasawa[6] proposed that H_2O participates in the transition state of formate decomposition by tilting the formate molecule. The appearance of this band is consistent with that proposal. Recently, Jacobs et al.[26] showed that increasing the Pt loading for Pt/ceria catalysts in the range of 0.5 to 5% had a pronounced impact on the WGS rate, and that the formate coverage during WGS was sparser for the more heavily loaded Pt catalysts. Recently, they showed that the transient formate decomposition rate was a direct function of the type and loading of metal promoter, with direct consequences in the WGS rate.[29] They proposed that the metal promoter may assist in decomposing the formate via enhanced metal-catalyzed H-abstraction.

Figure 8 provides a comparison of CO adsorption and WGS at 225 °C for Pt/hafnia and unpromoted hafnia. Note that Pt promotes the formation of the active bridging OH groups; CO acts as a probe molecule for these groups by reacting with them to form formate, and then the formate band intensities are significantly more intense for the Pt promoted catalyst. Moreover, during WGS, the CO_2 band is significantly higher for the case of the Pt promoted catalyst. This is consistent with the view that Pt assists in dehydrogenating formate in the catalytic cycle.

To explore the reactivity of the formate species further, the pseudostable formate was generated by CO adsorption to the H_2 activated catalyst, with cooling to 130 °C. Transient decomposition

dx.doi.org/10.1021/cs200231h |*ACS Catal.* 2011, 1, 1375–1383

of the formate (Figure 9) was followed in steam as a function of time. While some decrease occurs in the Pt-CO coverage as a function of time, the formate species rapidly disappear within a few minutes. During steaming, CO_2 was observed to evolve. Moreover, the low wavenumber band at 2846 cm^{-1} appears when H_2O is introduced, again in agreement with the proposal by Shido and Iwasawa[6] that H_2O promotes the decomposition of formate by participating in the transition state of forward formate decomposition. After steaming, Figure 10 indicates that the species present on the surface are likely mainly ν(OCO) stretching bands assigned to carbonate.

Taking into account that LTWGS occurs in Pt/HfO_2 via the associative pathway, with the adsorbed formate being an intermediate in the reaction, we were interested in verifying whether there may be a relationship between formate C−H bond strength and ionic radius, a periodic property, among the Group IV and related metal oxides, keeping in mind that C−H bond rupture has been suggested to be the rate limiting step.[6] Therefore, following the C−H bond frequencies of formate formed from adsorption of CO on the reduced catalyst by DRIFTS would give a good picture of whether or not a relationship may exist between formate reactivity and PRO metal ionic radius. Table 3 and Figure 11 indicate the main ν(C−H) stretching band from 1%Pt/HfO_2, combined with results from other Group IV and related catalysts obtained previously.[3,10,17,26] An interesting relationship is identified. The fact that a perfect relationship is not observed (e.g., Pt/HfO_2 is somewhat of an outlier) denotes that other factors, for example, crystallinity and variation in crystal structure, are also important. Nevertheless, the relationship observed suggests that larger ionic radii lead to a weaker (and thus more reactive) C−H bond. A proposed explanation, as illustrated in Figure 12, is that a weaker oxygen/metal bond (i.e., arising from the PRO possessing larger metallic ions) gives rise to stronger O−C bonds. The electron in the carbon participating in the covalent bond with H is then pulled toward the C−O system, resulting in a weaker C−H bond.

CONCLUSIONS

Catalysts composed of Pt and HfO_2 are active for WGS, and although the catalysts prepared in this work were not optimized, activities were within an order of magnitude of other Pt doped Group IV and related oxide catalysts (e.g., Pt dispersed on ZrO_2 and CeO_2). In DRIFTS, formates were observed to form during CO adsorption by reaction with bridging OH groups following catalyst activation. Because the formate band coverage was reaction rate limited (i.e., formates were turning over fast enough by forward decomposition to regulate their surface coverage) under steady state LTWGS, and because they were readily converted to carbonate species (precursor to CO_2) in the presence of steam at 130 °C, the results suggest that Pt/HfO_2 catalysts follow an associative pathway involving formate intermediates, as suggested for other catalysts containing Pt and an activated Group IV or related oxide. There is a relationship between the adsorbed formate C−H bond frequency and the crystallographic ionic radius of the metal in the partially reduced Group IV oxide, such that the larger the ionic radius, the lower is the frequency of the ν(CH) stretching mode of formate, and thus, the weaker is the C−H bond. Breaking of the C−H bond of formate is suggested to be the rate determining step of LTWGS.

AUTHOR INFORMATION

Corresponding Author

*Phone: (859) 257-0251. E-mail: burtron.davis@uky.edu.

REFERENCES

(1) Ratnasamy, C.; Wagner, J. P. *Catal. Rev.* **2009**, *51*, 325–440.
(2) Jacobs, G.; Davis, B. H. *Int. J. Hydrogen Energy* **2010**, *35*, 3522–3536.
(3) Jacobs, G.; Davis, B. H. In *Catalysis*; Spivey, J. J., Ed.; RSC Publishing: London, U.K., 2007; Vol. 20, p 122.
(4) Hilaire, S.; Wang, X.; Luo, T.; Gorte, R. J.; Wagner, J. *Appl. Catal., A* **2001**, *215*, 271–278.
(5) Li, Y.; Fu, Q.; Flytzani-Stephanopoulos, M. *Appl. Catal., B* **2000**, *27*, 179–191.
(6) Shido, T.; Iwasawa, Y. *J. Catal.* **1993**, *141*, 71–81.
(7) Jacobs, G.; Khalid, S.; Patterson, P. M.; Sparks, D. E.; Davis, B. H. *Appl. Catal., A* **2004**, *268*, 255–266.
(8) Jacobs, G.; Patterson, P. M.; Graham, U. M.; Sparks, D. E.; Davis, B. H. *Appl. Catal., A* **2004**, *269*, 63–73.
(9) Jacobs, G.; Patterson, P. M.; Graham, U. M.; Crawford, A. C.; Davis, B. H. *Int. J. Hydrogen Energy* **2005**, *30*, 1265–1276.
(10) Pigos, J. M.; Brooks, C. J.; Jacobs, G.; Davis, B. H. *Appl. Catal., A* **2007**, *319*, 47–57.
(11) Tabakova, T.; Idakiev, V.; Andreeva, D.; Mitov, I. *Appl. Catal., A* **2000**, *202*, 91–97.
(12) Idakiev, V.; Tabakova, T.; Naydenov, A.; Yuan, Z.-Y.; Su, B.-L. *Appl. Catal., B* **2006**, *63*, 178–186.
(13) Iida, H.; Igarashi, A. *Appl. Catal., A* **2006**, *303*, 48–55.
(14) Idakiev, V.; Tabakova, T.; Yuan, Z.-Y.; Su, B.-L. *Appl. Catal., A* **2004**, *270*, 135–141.
(15) Panagiotopoulou, P.; Kondarides, D. I. *J. Catal.* **2004**, *225*, 327–336.
(16) Iida, H.; Kondo, K.; Igarashi, A. *Catal. Commun.* **2006**, *7*, 240–244.
(17) Jacobs, G.; Crawford, A. C.; Williams, L.; Patterson, P. M.; Davis, B. H. *Appl. Catal., A* **2004**, *267*, 27–33.
(18) Jacobs, G.; Patterson, P. M.; Graham, U. M.; Crawford, A. C.; Dozier, A.; Davis, B. H. *J. Catal.* **2005**, *235*, 79–91.
(19) Tabakova, T.; Idakiev, V.; Tenchev, K.; Boccuzzi, F.; Manzoli, M.; Chiorino, A. *Appl. Catal., B* **2006**, *63*, 94–103.
(20) Sidgwick, N. V. *The Chemical Elements and Their Compounds*, Clarendon Press: Oxford, U.K., 1952.
(21) Eisenstein, O.; Hitchcock, P. B.; Hulkes, A. G.; Lappert, M. F.; Maron, L. *Chem. Commun.* **2007**, *17*, 1560–1561.
(22) Laing, M. *Found. Chem.* **2005**, *7*, 203–233.
(23) Krebs, R. E. In *The History and Use of Our Earth's Chemical Elements: A Reference Guide*; Greenwood Press: Westport, CT, 1998.
(24) Overbury, S.; Huntley, D.; Mullins, D.; Glavee, G. *Catal. Lett.* **1998**, *51*, 133–138.
(25) El Fallah, J.; Boujani, S.; Dexpert, H.; Kiennemann, A.; Majerns, J.; Touret, O.; Villain, F.; Le Normand, F. *J. Phys. Chem.* **1994**, *98*, 5522–5533.
(26) Jacobs, G.; Graham, U. M.; Chenu, E.; Patterson, P. M.; Dozier, A.; Davis, B. H. *J. Catal.* **2005**, *229*, 499–512.
(27) Jacobs, G.; Ricote, S.; Patterson, P. M.; Graham, U. M.; Dozier, A.; Khalid, S.; Rhodus, E.; Davis, B. H. *Appl. Catal., A* **2005**, *292*, 229–243.
(28) Moeller, T.; Kremers, H. E. *J. Phys. Chem.* **1994**, *48*, 395–406.
(29) Jacobs, G.; Ricote, S.; Graham, U. M.; Patterson, P. M.; Davis, B. H. *Catal. Today* **2005**, *106*, 259–264.
(30) Jacobs, G.; Ricote, S.; Davis, B. H. *Appl. Catal., A* **2006**, *302*, 14–21.
(31) Phatak, A. A.; Koryabkina, N.; Rai, S.; Ratts, J. L.; Ruettinger, W.; Farrauto, R. J.; Blau, G. E.; Delgass, W. N.; Ribeiro, F. H. *Catal. Today* **2007**, *123*, 224–234.
(32) Laachir, A.; Perrichon, V.; Badri, A.; Lamotte, J.; Catherine, E.; Lavalley, J. C.; El Fallah, J.; Hilaire, L.; Le Normand, F.; Quemere, E.; Sauvion, G. N.; Touret, O. *J. Chem. Soc., Faraday Trans.* **1991**, *87*, 1601–1609.